

THE BeppoSAX DEEP SURVEYS

P. Giommi^a, F. Fiore^{a, b}, D. Ricci^a, S. Molendi^c, M.C. Maccarone^d and A. Comastri^e

^aBeppoSAX Science Data Center, Rome, Italy

^bOsservatorio Astronomico di Roma, Monteporzio, Italy

^cIFCTR, CNR, Milano, Italy

^dIFCAI, CNR, Palermo, Italy

^eOsservatorio Astronomico di Bologna, Italy

We present the preliminary results of a survey that makes use of several deep exposures obtained with the X-Ray telescopes of the BeppoSAX satellite. The survey limiting sensitivity is $5 \times 10^{-14} \text{ erg cm}^{-2} \text{ s}^{-1}$ in the 2-10 keV band and $7 \times 10^{-14} \text{ erg cm}^{-2} \text{ s}^{-1}$ in the harder 5-10 keV band. We find that the 2-10 keV LogN-LogS is consistent with that determined in ASCA surveys. The counts in the 5-10 keV band imply either a very hard average spectral slope or the existence of a population of heavily absorbed sources that can hardly be detected in soft X-ray surveys. A sample of 83 serendipitous sources has been compiled from a systematic search in 50 MECS images. The analysis of the hardness ratio of this sample also implies very hard or heavily cutoff spectral shapes.

1. Introduction

Surveys of the high galactic latitude sky have greatly contributed to the solution of one of the most debated problems of X-ray astronomy: the nature of the X-ray background. It is now widely accepted that at least a substantial part of the apparently diffuse cosmic background is in fact due to the superposition of discrete extragalactic sources. A number of problems however still remain, the most notable one being the so called "spectral paradox" which reflects the fact that the measured spectral slope of the sources that are expected to make up the background is significantly steeper than that of the background itself. Solutions have been proposed in the framework of unified models for AGN which predict a large number of intrinsically obscured objects (Madau, Ghisellini and Fabian 1994, Comastri et al. 1995). These sources, however, can only be detected in sensitive hard X-ray surveys. Some work in this field has recently been done using ASCA data (Inoue et al. 1996, Georgantopoulos et al. 1997, Cagnoni, Della Ceca and Maccacaro 1998).

Here we present the preliminary results of a

survey that makes use of BeppoSAX imaging data. To date, twelve high galactic latitude deep exposures have been carried out with the imaging instruments of the BeppoSAX satellite (Boella et al. 1997a) for a total exposure of over 1.1 million seconds. We describe the results of a detailed study of an initial sample of six BeppoSAX deep X-ray images. This analysis allows us to estimate a new deep point in the 2-10 keV LogN-LogS and to derive for the first time the source counts in the harder 5-10 keV band. The results of a systematic analysis of 50 X-ray images, leading to a sizable sample of newly discovered hard X-ray selected sources are also presented.

2. BeppoSAX X-Ray imaging capabilities

The BeppoSAX satellite carries on board four X-ray telescopes, each one with a Gas Scintillation Proportional Counter (GSPC) as the focal plane detector. Three of these systems, the Medium Energy Concentrator Spectrometers (MECS, Boella et al. 1997b) are essentially identical and operate in the 1.3-10.5 keV band. The fourth system is known as the Low Energy Concentrator Spectrometer (LECS, Parmar et al.

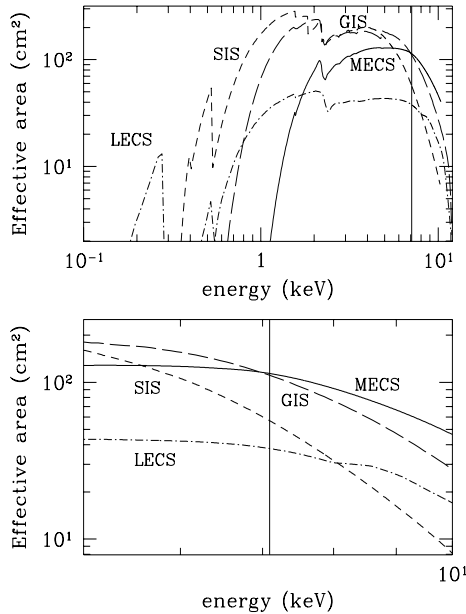


Figure 1. The effective areas of the BeppoSAX and ASCA imaging instruments. The bottom panel shows in more detail the region between 5 and 10 keV

1997) and operates between 0.1 and 10. keV extending the BeppoSAX spectral coverage down to the soft X-ray band.

The effective area of the LECS and MECS instruments are plotted in figure 1 together with those of the SIS and GIS detectors of the ASCA satellite (Tanaka et al. 1994).

The effective area of the ASCA GIS (two units) and SIS (two units) is higher than that of the MECS (three units) only at low energies. Above 5.5 and 7 keV, the MECS instruments have a larger collecting area and are therefore the best instruments available at the time of writing for surveys in the hard band.

One of the main advantages of the BeppoSAX imaging detectors over ASCA is the Point Spread Function (PSF) which is significantly sharper than that of the GIS or SIS, especially at high energy. A direct comparison is shown in figure 2

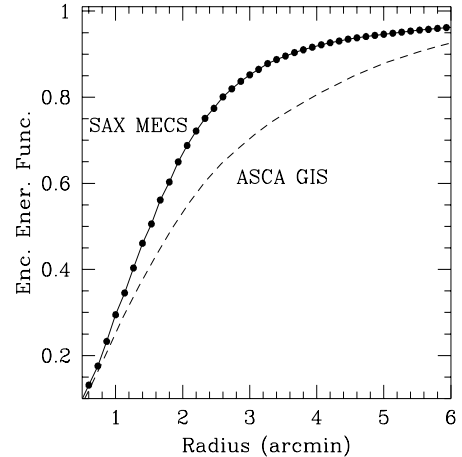


Figure 2. A comparison between the BeppoSAX MECS and the ASCA GIS Point Spread Functions

where the encircled energy function (for a typical spectral shape in the 2-10 keV band) of the BeppoSAX MECS is plotted together with that of the ASCA GIS. The radius where 50 % of the photons are collected are 1.4 and 1.9 arc minutes respectively. The comparison rapidly worsens for ASCA at larger radii where for instance to collect 80 % of the photons a radius of 3.6 arc minutes is needed compared to 2.6 arc minutes for BeppoSAX, corresponding to about a factor 2 in area. In addition, the MECS PSF in the soft band is largely instrument dominated and significantly improves at higher energies (up to about 6 keV) until scatter in the mirrors (which is much smaller than the spread due to the focal plane instruments at low energy) starts being the main contributor to the PSF. The difference in the response to a point source in the hard band is therefore even larger than that shown in figure 2.

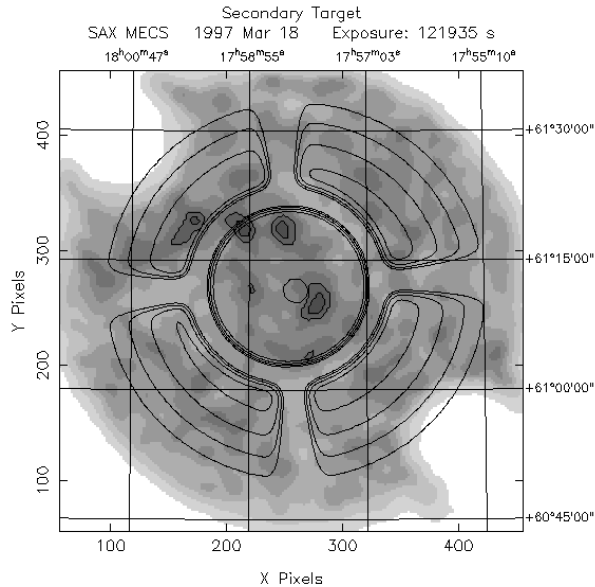


Figure 3. One of the BeppoSAX MECS deep fields. The effects of the window support structure are illustrated by the contour levels representing different levels of image sensitivity

A significantly better PSF has the obvious advantage of improving sensitivity (less background has to be subtracted to the signal) and reduces the effects of source confusion.

In the work reported we have only used data from the MECS instruments.

3. Observations

Table 1 gives the list of pointings that have been used for the analysis described in this paper. Column 1 gives the field name, column 2 the observation code in the BeppoSAX SDC archive, columns 3 and 4 give the Right Ascension and Declination (J2000.0) of the center of the field of view and column 5 gives the exposure time in seconds.

All observations have been carried out during the Science Verification Phase (SVP) or as secondary observations, that is when the MECS in-

struments were collecting data 90 degrees from a Wide Field Camera (WFC, Jager et al. 1997) primary pointing of the Galactic center region. In some cases deep exposures were accumulated while the satellite was recovering from minor technical problems and was therefore kept in the default pointing direction near Polaris.

All data used in this paper have been reprocessed using the most recently available reduction software. This ensures that systematic errors are kept to a minimum, that sensitivity is slightly improved over the one that could be achieved with earlier data, and that source positions are estimated using the best attitude calibration available to date.

4. Data Analysis

To search for faint sources in deep BeppoSAX X-ray images we have adopted a source detection procedure that is a variation of the detect routine included in the XIMAGE package (Giommi et al. 1991). The method consists in first convolving the X-ray image with a function of size similar to that of the MECS PSF (a wavelet function in this case) to smooth the image and increase contrast. As a second step a standard slide-cell detection method is used to locate count excesses above the local background. The statistics of each candidate detection is then accurately studied and the final net counts are estimated from the original (un-smoothed) image to preserve Poisson statistics. The background is calculated in a number of source-free boxes near the position of the candidate detection and is rescaled taking into account of spatial variations of the MECS background. To maximize sensitivity the size of the box used for flux estimation is chosen to be that where the signal to noise ratio is expected to be maximum given the local background, source intensity and local PSF.

Extensive Monte Carlo simulations made using the BeppoSAX on-line simulator, show that this source detection method is fast and highly sensitive to point sources even in presence of some source confusion. The method is also statistically robust since final acceptance and flux estimation on each detection is simply based on

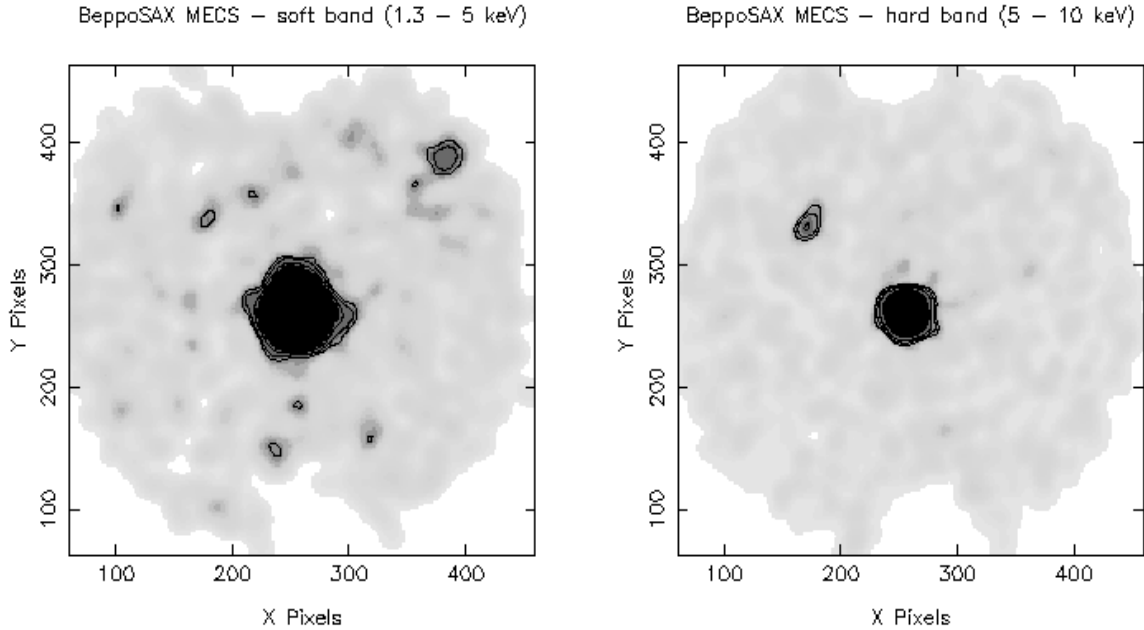


Figure 4. Soft (1.3-5 keV) and hard (5-10 keV) MECS images of the same field. Note that the soft source near the edge of the FOV on the top right part of the plot is barely visible in the hard band, while the source north east of the target in the hard image is very faint in the 1.3-5 keV band. Note also that the PSF in the hard band is significantly sharper than that in the 1.3-5 keV band

Poisson statistics and does not require any time consuming fitting procedures which, especially in case of weak signal, may not always be stable.

4.1. Source detection in the 2-10 keV band

The MECS X-Ray images have a circular field of view with radius of approximately 25 arcminutes.

The sensitivity to X-ray sources is a fairly strong function of the position in the image. Several factors contribute to this complex dependency. Figure 3 shows one of the deep fields used in our survey shown together with its sensitivity map overlaid as a set of contour levels. The most notable feature is the obscuration due to the detector window support structure (also known as the strongback) that is clearly visible in the sensitivity contours. The strongback is made of 600

microns of Beryllium and absorbs most of the X-rays below 5 keV. The two small empty regions near edge of the field of view on the top left and bottom right part of the image, are due to the removal of the area affected by the on-board calibration sources. Another cause of the sensitivity dependency on distance from the center is the well known vignetting effect which for the MECS detectors can be as high as a factor 3.5 at very large off axis angles. Finally the PSF also degrades with distance from the center; however, since the spread in the MECS is dominated by detector effects (at least up to about 6 keV), this is a smaller problem than in most other X-ray telescopes.

To avoid complications due to complex variations in sensitivity across the field of view for our survey we only consider the central region of 9

Table 1
BeppoSAX Deep Fields

Field	Observation_code	RA	DEC	Exposure time
WFC Secondary	00001003	17 30 42.	+60 55 33	65841
WFC Secondary	00001005	16 33 43.	+59 44 13	97937
WFC Secondary	00001007	18 04 03.	+61 08 43	116720
WFC Secondary	00001008	17 58 15.	+61 10 19	118969
WFC Secondary	00001009	18 19 50.	+60 56 37	114574
Polaris 1	00001011	01 38 18.	+89 13 51	115498

arcminutes radius where sensitivity does not vary more than a few percent (see figure 3). Full exposure map corrections were applied to all images considered. The exposure in all fields listed in table 1 is sufficiently long to guarantee a theoretical sensitivity (in absence of source confusion) of $2 - 3 \times 10^{-14} \text{ erg cm}^{-2} \text{ s}^{-1}$. However, because of source confusion problems (see below) we decided to limit our survey to a sensitivity of $5 \times 10^{-14} \text{ erg cm}^{-2} \text{ s}^{-1}$. Each field therefore contributes to our survey with a constant area equal to 0.07 square degrees with fixed sensitivity of $5 \times 10^{-14} \text{ erg cm}^{-2} \text{ s}^{-1}$.

Images were accumulated in the 2-10 keV band for all the six pointings listed in table 1 and the detection algorithm described above was run on all data.

Sources were accepted according to the following criteria.

- 1) The off-axis angle is less or equal to 9 arcminutes;
- 2) Statistical probability that the source is a fluctuation of the local background is less than 1×10^{-4} . This implies that less than one spurious source is expected in the entire survey.
- 3) The count rate corresponds to a 2-10 keV flux higher or equal to $5 \times 10^{-14} \text{ erg cm}^{-2} \text{ s}^{-1}$ assuming a power law spectrum with an energy slope of 0.7.

The analysis of all BeppoSAX deep fields was also carried out on the soft (1.3-5 keV), hard (5-10 keV) band. This ensures that sources with very soft or hard spectrum (figure 4) are not missed.

5. The 2-10 keV LogN-LogS

Since the sensitivity limit was fixed to the same value in all images the estimation of the source counts in our survey is simply a single point in the LogN-LogS plane.

Nineteen sources were detected in the 0.42 square degrees of the survey corresponding to a density of 45 ± 10 sources/sq degree with flux equal or larger than $5 \times 10^{-14} \text{ erg cm}^{-2} \text{ s}^{-1}$.

At present most of these sources are unidentified. Figure 5 shows the MECS deep fields point in the 2-10 keV LogN-LogS plane together with the results of ASCA (Georgantopoulos et al. 1997, Cagnoni et al. 1998), Ginga (Kondo et al. 1991) and HEAO1 (Piccinotti et al. 1982). The BeppoSAX counts are clearly in good agreement with the results of ASCA.

6. Simulations and the source confusion problem

To address the problem of source confusion and biases at faint fluxes near the detection limit (see e.g. Hasinger et al. 1998), we simulated a large number of MECS deep fields using the BeppoSAX on-line data simulator described below.

6.1. The BeppoSAX simulator

The BeppoSAX on-line X-ray data simulator (<http://www.sdc.asi.it/simulator>) is a facility provided by the BeppoSAX Science Data Center (Giommi & Fiore 1997) that can be used to make detailed simulations of LECS and MECS X-ray imaging data. This software generates X-ray sources randomly distributed across the image following a LogN-LogS equal to that determined using ASCA data by Cagnoni et al (1998).

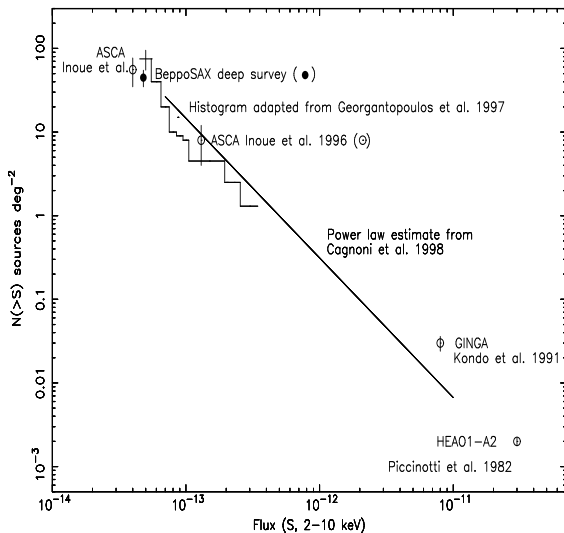


Figure 5. The 2-10 keV LogN-LogS as estimated with various X-ray astronomy satellites. The BeppoSAX deep survey point at $S=5 \times 10^{-14} \text{ erg cm}^{-2} \text{ s}^{-1}$ is consistent with other measurements.

Detector effects including position and energy dependent PSF and telescope vignetting, are fully taken into account. The format of the output files is identical to that of LECS or MECS science archive data so that the same analysis software and procedures can be used for simulated and real data.

6.2. Simulation runs

Fifty deep fields with exposures of 100,000 seconds each, were generated and subsequently analyzed following the same method used for the survey. This resulted in the detection of a relatively large sample of sources which was then used to estimate the source counts at different flux limits. These estimates were finally compared to the LogN-LogS used as input for the simulation.

No significant bias in the estimation of the LogN-LogS could be found down to a flux of ap-

proximately $5 \times 10^{-14} \text{ erg cm}^{-2} \text{ s}^{-1}$. At lower flux levels several sources could still be detected but in this regime source confusion causes severe problems in the determination of source flux and accurate positions (see also the results of Hasinger et al. 1998).

7. Hard sources

The results in the 2-10 keV band encouraged us to extend our analysis of BeppoSAX deep fields to the hard band and to estimate the source counts between 5 and 10 keV. The BeppoSAX MECS are well suited for this determination since their effective area peaks at around 5-6 keV (see figure 1) and the PSF in the hard band is sharper than that in the full 2-10 keV band. Source confusion is not a major problem anymore.

7.1. The hard (5-10 keV) LogN-LogS

We have repeated the analysis carried out for the 2-10 keV data on images accumulated in the harder 5-10 keV band. The sensitivity limit, set equal for all six images as in the case of the 2-10 keV band, was $7 \times 10^{-14} \text{ erg cm}^{-2} \text{ s}^{-1}$. Because of possible small systematic effects and of the uncertainty in the knowledge of the sources spectral slope we conservatively associate an uncertainty of 1×10^{-14} in the flux limit.

This analysis has led to the detection of 8 sources yielding a density of 19 ± 7 sources/sq degree.

Figure 6 plots the BeppoSAX (5-10 keV) source density at $7 \times 10^{-14} \text{ erg cm}^{-2} \text{ s}^{-1}$ in the LogN-LogS plane. Since no results from other satellites are available yet in this band, comparison with other data can only be done by extrapolating results obtained in softer bands assuming different spectral slopes. The solid line shown in figure 6 represents the 5-10 keV LogN-LogS as expected from the Cagnoni et al (1998) counts assuming a spectral slope of $\alpha = 0.4$. The BeppoSAX counts are about a factor 2 higher than expected, indicating that a very flat ($\alpha \leq 0.2$), and most probably unphysical, average source spectrum must be assumed. Alternatively, a population of heavily cutoff sources could explain the difference.

The still relatively large statistical uncertain-

ties, however do not allow strong conclusions and more data are necessary to confirm these early results. The analysis of all existing BeppoSAX deep fields will contribute to address this point.

The nature of the BeppoSAX hard X-ray sources is still unknown. An important contribution is expected from obscured type 2 objects as predicted in the AGNs synthesis models for the hard X-ray background (Madau Ghisellini and Fabian 1994, Comastri et al. 1995). These sources can hardly be detected in the soft X-rays even at the faintest ROSAT limit while in harder energy bands they should become detectable. To further investigate this possibility we have computed the source space density in the 5–10 keV band predicted by the Comastri et al. (1995) model (figure 7). The dotted line represent the contribution of unabsorbed type 1 objects (e.g. Seyfert 1 galaxies and quasars), while the solid line gives the summed contribution of unabsorbed and absorbed objects. The model predictions are consistent (at the 2σ level) with the BeppoSAX observations.

The small discrepancy between the observed and predicted source surface density may be due to several factors, including poor statistics. The model predictions have been computed assuming for the AGN luminosity function and cosmic evolution the best fit parameters derived by ROSAT (Boyle et al. 1993), which may not be appropriate especially for the highly absorbed sources. The contamination of non-AGN sources (which are not included in the model) to the observed counts could be important given the relatively low number of hard X-ray sources (eight). A different explanation would imply the contribution of a new class of very hard X-ray sources which have been missed by previous surveys. A more detailed discussion of these points is deferred to a future paper.

8. Hardness ratio analysis

Figure 4 shows the soft (1.3–4.0 keV) and hard (4–10 keV) X-ray image of a MECS observation where two serendipitous sources with different spectral shape have been detected. The source near the edge at the top right of the soft image is

only detected in the soft band, while most of the photons from the source to the northeast of the target are detected above 4 keV.

Similarly, the sources that we have detected in our survey show a variety of spectral slopes, ranging from soft stellar like spectra to very hard ones where nearly all the photons are detected in the hard band.

To study this spectral variety in a quantitative way we have conducted a systematic search for serendipitous sources in a sample of 50 MECS images (see Fiore et al. 1998) selected among SVP observations or from fields where the SAX team or one of the authors of this work is the PI. This search led to the detection of 83 serendipitous sources. For each detection we have estimated the hardness ratio (defined as $HR=(S-H)/(S+H)$, where S are the net counts in the 1.3–4.5 keV band and H are the counts in the 4.5–10. keV band).

Figure 8 plots the hardness ratios as a function of source total count-rate. The solid triangles represent the serendipitous sources discussed above, (the error bars are not plotted but typically are of the order of 0.2–0.3). Open circles represent a set of pointed AGN (observed during SVP or that are AO1 observations where one of the authors of this work is a PI or one of the main co-investigators); filled circles are pointed sources which are well known to be intrinsically absorbed sources. The scale on the right vertical axis shows the equivalent (energy) spectral slope for an assumed power law spectrum. We see that the hardness ratio of the serendipitous sources is systematically lower than that of pointed (and unabsorbed) AGN, with typical values corresponding to very flat spectral slopes (α around 0!). The fact that there are very few serendipitous sources with hardness ratio similar to that of the pointed AGN is a simple selection effect: at very low count rates, near the detection limit, a soft source would not be detected in the hard band and therefore no hardness ratio for it can be estimated. From figure 8 we can conclude that a substantial population of very hard (or very absorbed) serendipitous sources has been detected, consistently with the expectations from the LogN-LogS results.

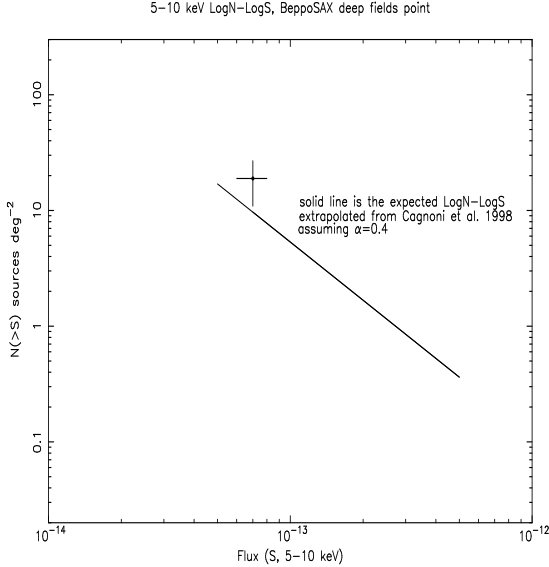


Figure 6. The 5-10 keV BeppoSAX counts compared to the expectations from the ASCA LogN-LogS assuming an average (energy) spectral slope $\alpha = 0.4$

9. Conclusions

We have presented early results from a project that deals with a relatively deep survey of the high galactic latitude sky in the 2-10 keV and 5-10 keV bands. The data used are six deep observations made with the imaging instruments of the BeppoSAX satellite.

The results in the 2-10 keV band are in good agreement with those found in the ASCA deep surveys. This confirms that at a flux of $5 \times 10^{-14} \text{ erg cm}^{-2} \text{ s}^{-1}$ about 30% of the cosmic background is resolved in point sources and that there is an excess of hard X-ray sources compared to the predictions derived from the ROSAT 0.5-2. keV LogN-LogS (Hasinger et al. 1993, Inoue et al. 1996, Geogantopoulos et al. 1997). This last conclusion is further strengthened by the high number of sources found in the hard 5-10 keV band. This result can be explained assuming the existence of a population of objects that could not

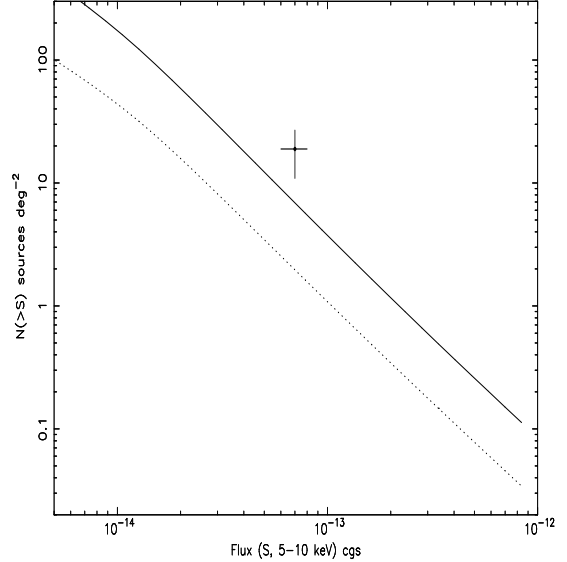


Figure 7. The prediction of the Comastri et al (1995) model (solid line) compared to the 5-10 keV source counts from the BeppoSAX deep survey. The dotted line represents the contribution of unabsorbed AGN.

be detected by ROSAT but is contributing to the BeppoSAX space density. Several hard sources have indeed been detected by us as serendipitous sources in a set of 50 MECS X-ray images.

The source surface density at the BeppoSAX flux limit is in overall agreement with the expectation of the AGN synthesis models for the XRB.

The population of hard sources could include Seyfert 2 galaxies with high intrinsic absorption (NH around 1×10^{23}), as predicted by unified models for AGN (e.g. Antonucci 1993) and consistent with BeppoSAX direct observations (Salvati et al. 1997). A significant test for these models would be the comparison with the optical identifications of the BeppoSAX hard X-ray sources. Deeper observations with the next generation of X-ray observatories with good angu-

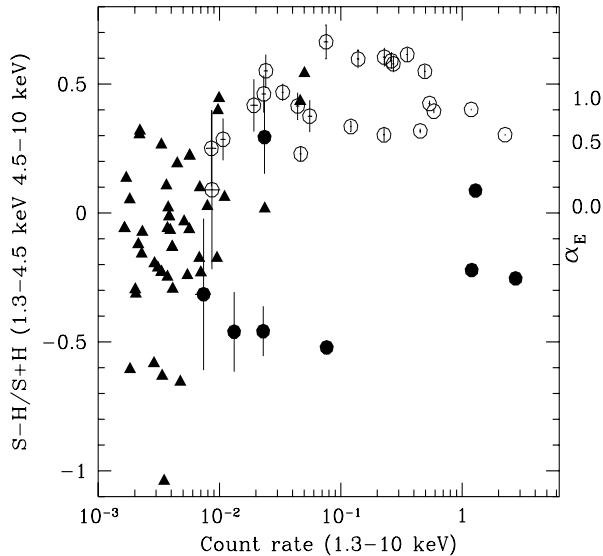


Figure 8. The hardness ratios of MECS serendipitous sources (filled triangles) plotted as a function of count rate. For comparison the HR of several pointed AGN (open circles) and highly absorbed targets (filled circles).

lar resolution and high spectral sensitivity in the hard X-ray band (i.e. AXAF and XMM) will also allow to tighten the constraints on the nature of the weak hard X-ray sources and in turn provide a definitive answer on the origin of the X-ray background.

10. Acknowledgments

We thank T. Maccacaro, and M. Salvati for providing some of their BeppoSAX results in advance of publication.

REFERENCES

1. Antonucci, R. In: Annual review of astronomy and astrophysics. 31, 473
2. Boella G. Butler, R. C., Perola, G. C., Piro,

- L., Scarsi, L., Bleeker, J. A. M 1997a A&AS, 122, 299
3. Boella G. et al. 1997b A&AS, 122, 327
4. Boyle B.J. et al. 1993, MNRAS 260, 49
5. Cagnoni I.; Della Ceca, R.; Maccacaro, T., 1998, ApJ 493, 54
6. Comastri A., Setti, G., Zamorani, G., Hasinger, G., 1995 A&A, 296, 1
7. Hasinger G., Burg, R., Giacconi, R., Hartner, G., Schmidt, M., Trümper, J., Zamorani, G. 1993, A&A 275, 1.
8. Hasinger G., Burg, R., Giacconi, Schmidt, M., Trümper, J., Zamorani, G. 1998, A&A 329, 482
9. Inoue H., Kii, T., Ogasaka, Y., Takahashi, T., Ueda, Y. 1996 Pro. 'Röntgenstrahlung from the Universe', eds. Zimmermann, H.U. Trümper, J., and Yorke, H.; MPE Report 263, p. 323-326
10. Fiore F., Ricci D., Giommi P., Matt G., Molendi S., 1998, these proceedings.
11. Jager R. et al. 1997 A&AS, 125, 557
12. Kondo et al. 1991
13. Georgantopoulos I., et al. 1997 MNRAS, 291, 203.
14. Giommi, P., Angelini, L., Jacobs, P. & Tagliferri G. 1992 in "Astronomical Data Analysis Software and Systems I", D.M.Worrall, C. Biemesderfer and J. Barnes eds, 1991, A.S.P. Conf. Ser. 25, 100
15. Giommi P., & Fiore F. 1997, Proc. of "5th International Workshop on Data Analysis in Astronomy, Erice.
16. Madau, P., Ghisellini, G. & Fabian, A.C., 1994 MNRAS, 270, L17
17. Parmar A. et al. 1997 A&AS, 122, 309
18. Piccinotti G., Mushotzky, R. F., Boldt, E. A., Holt, S. S., Marshall, F. E., Serlemitsos, P. J., Shafer, R. A. 1982, APJ 253, 485.
19. Salvati M., Bassani, L., Della Ceca, R., Maiolino, R., Matt, G., & Zamorani, G. 1997.
20. Tanaka Y., Inoue H., Holt S.S., 1994, PASJ 46, 137.